Available online at www.sciencedirect.com
ScienceDirect
Dyes and Pigments 74 (2007) 483–489
DYES and PIGMENTS
www.elsevier.com/locate/dyepig

Water and alcohol-soluble octakis-metalloporphyrazines bearing sulfanyl polyetherol substituents: Synthesis, spectroscopy and electrochemistry

Mehmet Kandaz [a,*], Ali Rıza Özkaya [b], Atıf Koca [c], Bekir Salih [d]

[a] Department of Chemistry, Sakarya University, 54140 Esentepe, Sakarya, Turkey
[b] Department of Chemistry, Faculty of Science and Letters, Marmara University, 34722 Kadıköy, Istanbul, Turkey
[c] Chemical Engineering Department, Engineering Faculty, Marmara University, 34722 Göztepe, Istanbul, Turkey
[d] Department of Chemistry, Faculty of Science, Hacettepe University, Beytepe Campus, Ankara 06532, Turkey

Received 9 March 2006; accepted 21 March 2006
Available online 19 May 2006

Abstract

Water-soluble metalloporphyrazines (**2**, **3**, and **4**) bearing peripherally functionalized bis[thioethoxy(ethoxy)ethanol] moieties have been prepared from the corresponding [2H]-2,3,7,8,12,13,17,18-octakis{2-[2-2-hydroxyethoxy)ethoxy]-ethylthio}porphyrazine and appropriate metal salts [$Zn(acac)_2$, $CoCl_2$, $MnCl_2$] in non-aqueous polar solvents such as, alcohol and THF. Multifunctional polyetherolsulfanyl peripheral sites, the exocyclic site of porphyrazines, serve as weak interacting ionophore in a number of metal ions, such as Ag^I and Pd^{II}. The reactivity of the peripheral groups of MPzs was tested by spectrophotometric titration by Ag^I and Pd^{II}. The titration resulted in the formation of intractable less soluble black and dark-blue polynuclear porphyrazine complexes. The new compounds have been characterized by elemental analysis, FTIR, ^1H NMR, UV–vis and MS (MALDI-TOF). The voltammetric investigation of the complexes showed common ligand and metal-based redox processes.

Keywords: Water-soluble porphyrazine; Zinc; cobalt and manganese; Polyetherol; Aggregates; Metal sensor; Electrochemistry; Cyclic voltammetry

1. Introduction

Purpose-designed peripherally functionalized porphyrazines fused directly to the β,β-position of pyrroles have the potential for a wide range of high-technological applications, such as electron transfer, magnetic interactions, photodynamic therapy and in biomimetic chemistry [1–5]. A decisive disadvantage of porphyrazines/phthalocyanines is their low solubility in organic solvents [6,7]. The solubility of these compounds can be increased, however, by introducing bulky or long chain groups, e.g. alkyl, alkoxy, quaternized ammonium, sulfo, sulfonamide, polyalcohol, etc. into the peripheral sites of the porphyrazines/phthalocyanines [8–12]. The advantage of using soluble porphyrazines for high-technological applications, in contrast to the insoluble ones, is the possibility of reaching high degrees of purification by column chromatography or crystallization [13–16]. The size of the substituent is not the only criterion for the solubility of the substituted porphyrazines; the symmetry caused by the substituents in periphery and metal in the core is also important [17–20]. The moieties enabling solubility of complexes in water involve generally heteroatoms, such as N, S, and O, appended to the porphyrazine or phthalocyanine ring and thus these complexes can be designed to bind exocyclic metal ions [21–25]. These moieties introduce an additional electronic, optical or redox properties, or even confer a desired solubility [23–25].

We have been investigating recently the functional symmetrical oximes and symmetrical or unsymmetrical phthalocyanine/porphyrazines in the form of $M[Pz(A)_4]$ or $M[PzA_n{:}B_{4-n}]$ in which A and B represent functional groups appended

* Corresponding author. Tel.: +90 264 2760237; fax: +90 264 2762059.
E-mail address: mkandaz@sakarya.edu.tr (M. Kandaz).

0143-7208/$ - see front matter © 2006 Elsevier Ltd. All rights reserved.
doi:10.1016/j.dyepig.2006.03.014

directly to the β-position of the pyrroles in the macrocycle, and M represents a metal ion coordinated in the macrocyclic core [26–31]. Peripheral functionalized porphyrazines/phthalocyanines are prepared by the template cyclization of maleonitrile and/or phthalonitrile derivatives. The ability to vary the types and the number (*n*) of A and B allows for even greater control over the physical properties of the macrocycles. Functional groups attached in this way have stronger coupling ability to the macrocycle core than those attached to the fused benzo ring of the porphyrazines/phthalocyanines, and therefore exert a greater effect on magnetic and physical properties [8,25,32,33].

In this paper, as a part of our previous studies, development of functionalized *vic*-dioxime porphyrazines/phthalocyanines with multiple metal ion binding sites [8,20,26–28], we report the synthesis, characterization and electrochemistry of metalloporphyrazines that have eight peripheral bis[thioethoxy-(ethoxy)ethanol] moieties.

2. Experimental

Bis(disodium) maleonitriledithiolate (Na_2MNT) and [2H]-2,3,7,8,12,13,17,18-octakis{2–2-(2-hydroxyethoxy]ethoxy]-ethylthio}porphyrazine were prepared according to the procedures [15,34]. All organic solvents were dried and distilled. All reagents were freshly distilled or recrystallized and dried under reduced pressure. FTIR spectra (thin film) were recorded on a ATI Unicom-Mattson 1000 spectrophotometer. Elemental analysis (C, H, and N) was performed at the Instrumental Analysis Laboratory of TUBITAK Gebze Research Center and Marmara University. Electronic (UV–vis) absorption spectra were recorded on a Unicam UV2 spectrophotometer. Nuclear magnetic resonance spectra were recorded on a Bruker (200 MHz). Chromatography was performed with silica gel (Merck grade 60 and sephadex) from Aldrich. The homogeneity of the products was tested in each step by TLC (SiO_2, $CHCl_3$ and methanol). Mass spectra were acquired on a Voyager-DE™ PRO MALDI-TOF mass spectrometer (Applied Biosystems, USA) equipped with a nitrogen UV-Laser operating at 337 nm. Spectra were recorded in reflectron mode with an average of 50 shots (Figs. 1 and 2). 3-Indole acrylic acid (IAA) (20 mg/mL in acetonitrile) and α-cyano-4-hydroxy cinnamic acid (ACCA) (15 mg/mL, 1:1 water–acetonitrile), MALDI matrices, for **1**, **2** and **3** were prepared. MALDI samples were prepared by mixing complexes (2 mg/mL in acetonitrile) with matrix solution (1/10 v/v) in a 0.5 mL eppendorf® micro tube. Finally 1 μL of this mixture was deposited on the sample plate, dried at room temperature and then analyzed.

Cyclic voltammetric and controlled potential coulometric (CPC) measurements were carried out with Princeton Applied Research Model 273 potentiostat controlled by an external PC, using the computer program HEADSTRT utilizing a three electrode configuration at 25 °C. The origin 5.0 graph program was used to evaluate the HEADSTRT data, to draw voltammograms and analyze them. A Pt wire served as the counter electrode. A saturated calomel electrode (SCE) was employed as the reference electrode and was separated from the bulk of the solution by a glass bridge. The working electrode was a Pt plate with an area of 1.0 cm^2. A solution of 0.1 mol dm^{-3} tetrabutylammoniumperchlorate (TBAP) in extra pure DMSO was employed as the supporting electrolyte. High purity N_2 was used for deaeration at least 15 min prior to each run. For CPC studies, a Pt gauze working electrode (10.5 cm^2 surface area), a platinum wire counter electrode separated by a glass bridge, saturated calomel reference electrode, and a model 377/12 synchronous stirrer were used.

*2.1. [Zn]2,3,7,8,12,13,17,18-octakis {2-2-(2-hydroxyethoxy]ethoxy]-ethylthio}porphyrazine (**1**)*

Free-base porphyrazine, [2H]-2,3,7,8,12,13,17,18-octakis{2-(2-(2-hydroxyethoxy]ethoxy]-ethylthio}porphyrazine (0.200 g, 0.130 mmol), and anhydrous $Zn(OAc)_2$ (0.024 g, 0.130 mmol) in a mixture of $CHCl_3$ (15.0 cm^3) and MeOH (7.5 cm^3) solvents were heated to reflux temperature with stirring for 4–6 h under nitrogen. Then, the solvent mixture was removed by rotary evaporation. The green-blue residue was

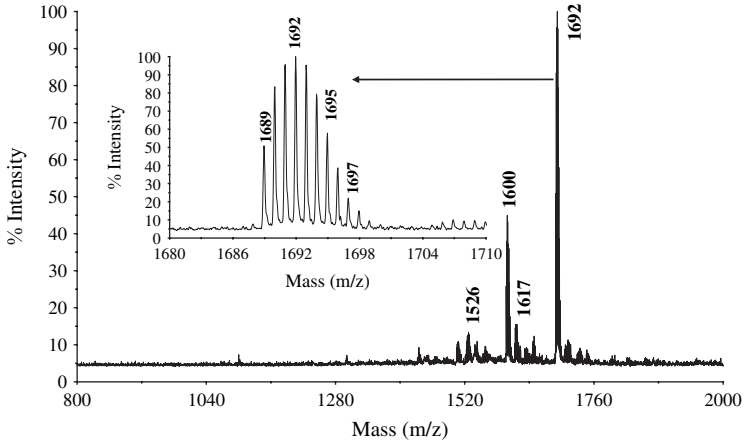

Fig. 1. Positive ion and reflectron mode MALDI-MS spectrum of **1** was obtained in α-cyano cinnamic acid MALDI matrix using nitrogen laser accumulating 50 laser shots. Inset spectrum shows expanded molecular mass region of the complex.

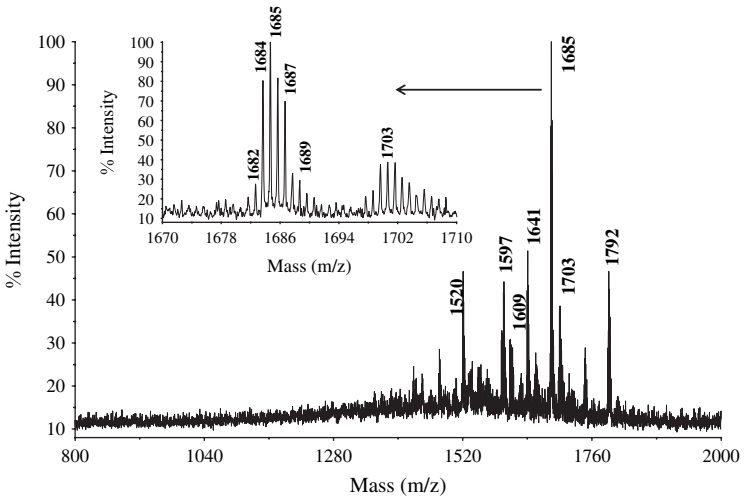

Fig. 2. Positive ion and reflectron mode MALDI-MS spectrum of **2** was obtained in α-cyano cinnamic acid MALDI matrix using nitrogen laser accumulating 50 laser shots. Inset spectrum shows expanded molecular mass region of the complex.

taken up in $CHCl_3$ and filtered. The volume was reduced to about 5 cm^3 by rotary evaporation, and the resulting desired product was further purified by silica gel chromatography (5/2 v/v; $CHCl_3$:MeOH), affording 0.058 g (27.69%) of a green-blue oily zinc–porphyrazine. FTIR ν_{max} (cm^{-1}): 3363, 3263, 2955, 2926, 2856, 1718 (w), 1652 (st), 1457, 1389, 1452, 1270, 1185, 1104, 1038, 967, 712. ^1H NMR (300 MHz, $CDCl_3$) δ: 2.07 (br s, 8H, $-CH_2OH$ D_2O-exchangeable), 3.19 (br t, 16H, $-CH_2-S$), 3.44–3.60 (m, 32H, ($2\times OCH_2-CH_2O$)), 4.01 (t, 16H), 4.31 (t, 16H, CH_2–OH). UV–vis ($CHCl_3$): λ_{max}/nm (log ε): 374, 506 (sh), 617 (sh), 668. MS (MALDI-TOF, α-cyano-4-hydroxy cinnamic acid (CHCA) as matrix): (100%) *m/z*: 1689.98 $[M+H]^+$, 1690.96, 1691.96, 1692.96, 1693, 1694, 1695, 1696, 1697 and 1698 representing the isotopic distribution of the metal, carbon and different oxidation states, and also 1711.93 (5%).

2.2. [Mn]2,3,7,8,12,13,17,18-octakis {2-2-(2-hydroxyethoxy]ethoxy]-ethylthio}porphyrazine (*2*)

Compound **3** was prepared by the same procedure as described for **1** starting from [2H]-3,7,8,12,13,17,18-octakis{2-(2-(2-hydroxyethoxy]ethoxy]-ethylthio}porphyrazine (0.200 g, 0.130 mmol) and anhydrous excess $MnCl_2$ (ca 0.016 g, 0.130 mmol). The blue residue was taken up in $CHCl_3$ and filtered. The volume was reduced to about 2–3 cm^3 by rotary evaporation, and the resulting desired product was purified by silica gel chromatography (5/2 v/v; $CHCl_3$:MeOH), affording 0.045 g (20.62%) of a green-blue oily manganese porphyrazine. FTIR ν_{max} (cm^{-1}): 3384, 3240, 2986, 2955, 2885, 1710 (w), 1473,1392, 1252, 1105,1065, 1037, 954, 838, 795, 666, 585. UV–vis ($CHCl_3$): λ_{max} (nm): 349, 469 (sh), 580 (sh), 641. MS (MALDI-TOF, α-cyano-4-hydroxy cinnamic acid (CHCA) as matrix): (100%) *m/z*: 1681.87 $[M+H]^+$, 1682.93, 1683.94, 1684.93, 1685.93 representing the isotopic distribution of the metal, carbon and different oxidation states, and also the peak groups at 1705.87 (25%) $[M+Na]^+$ with isotropic distribution of metal.

2.3. [Co]2,3,7,8,12,13,17,18-octakis {2-2-(2-hydroxyethoxy]ethoxy]-ethylthio}porphyrazine (*3*)

The free-base porphyrazine (0.200 g, 0.130 mmol) and anhydrous $Co(OAc)_2$ (0.0011 g, 0.130 mmol) in ethylene glycol (10.0 cm^3) solvent were heated to reflux temperature with stirring for 4–6 h under nitrogen. Then, the mixture was cooled to room temperature and the solvent was removed by rotary evaporation. The blue residue was taken up in $CHCl_3$ and filtered. The volume was reduced to about 2–3 cm^3 by rotary evaporation, and the resulting desired product was further purified by silica gel chromatography (5/1 v/v; $CHCl_3$:MeOH), affording 0.066 g (30.16%) of a green-blue oily cobalt porphyrazine. FTIR ν_{max} (cm^{-1}): 3399, 2980, 2928, 2873, 1716 (w), 1654, 1507, 1473, 1394, 1249, 1104, 1066, 1038. UV–vis ($CHCl_3$): λ_{max} (nm): 349, 469 (sh), 580 (sh), 641. MS (MALDI-TOF, α-cyano-4-hydroxy cinnamic acid (CHCA) as matrix): (100%) *m/z*: 1684.85, 1685.85, 1686.73 isotopic distribution, 1703.85 (7%) $[M+H_2O]^+$.

3. Results and discussion

3.1. Synthesis and characterization

Functionalized metalloporphyrazines are typically synthesized by the templated cyclization of the corresponding maleonitrile and appropriate anhydrous metal salts as shown in Scheme 1. The reaction of free porphyrazine with anhydrous $Zn(OAc)_2$, $MnCl_2$, and $CoCl_2$ metal salts gave internally metallated metalloporphyrazines (**1**, **2**, and **3**) using a standard procedure [8,13,15]. In contrast with phthalocyanines, insertion of the metal ions into the porphyrazine core is remarkably fast at room temperature, occurring in about 4–6 h [6,7]. During the synthesis and purification of **2** and **3**, the incorporated metal ions were not oxidized from Mn^{II} to Mn^{III} and from Co^{II} to Co^{III} [8]. The most obvious feature of the newly synthesized metalloporphyrazines is their high solubility in common organic solvents, e.g. $CHCl_3$, CH_2Cl_3, THF, acetone, DMF,

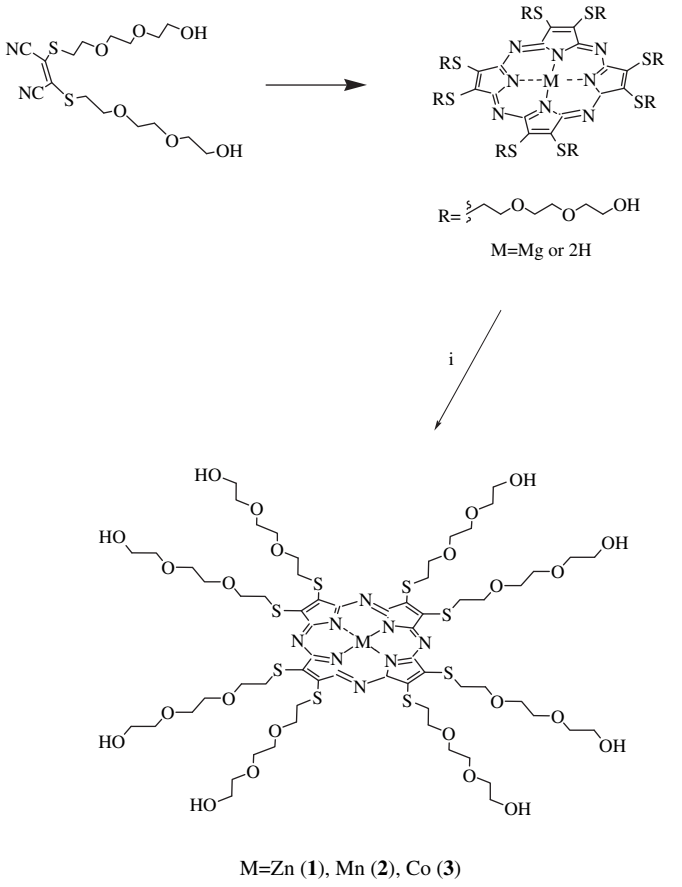

Scheme 1. Synthesis of the porphyrazines **1**–**3**.

DMSO and even in water. Purification steps were tedious because of peripheral polarities. The blue-green cyclotetramerization products, MPz's (M = Zn, Mn and Co) were purified by column chromatography in moderate yield (27.69% for **1**, 20.62% for **2** and 30.16% for **3**). Elemental analysis results and the spectral data (^{1}H NMR, FTIR, and MALDI-TOF MS) of all the new products are consistent with the assigned formulations.

The FTIR spectra were used to identify substituents on the periphery of each metalloporphyrazine core. Characteristic IR stretching vibrations attributed to the $-CH_2OH$, $-CH$(aliphatic), R–O–R and CH_2–S pyrroline groups of the bis[ethoxy-(ethoxy)ethanol] chains were observed at 3260, 2973–2852, 1260, and 1100 cm^{-1}, respectively.

The ^{1}H NMR spectra of **1** indicate deshielding of aliphatic protons of coordinated ligand, bis{2-[2-(2-hydroxyethoxy)-ethoxy]-ethylthio}maleonitrile upon metal coordination. The singlet at −1.34 ppm, corresponding to NH in the NMR spectrum of free-base, 2H [Pz(S–$(CH_2O)_2CH_2OH)_4$], disappeared after conversion to metalloporphyrazines. However, the existence of deuterium-exchangeable CH_2OH heteroatom signal at 2.07 ppm was observed as a new broad singlet again with a slight shift. The signals for the deuterium-exchangeable CH_2OH group at 4.37 ppm disappeared upon addition of D_2O. As compared to the spectra of the free-base porphyrazine, the shifts and changes in the intensity of certain peaks in the ^{1}H NMR spectra of **1** are consistent with the metallation. The signals for methylene protons in **1** are similar to those of free-base with small shifts.

Protonated molecular ion peak of **1** was observed at 1689 Da that was exactly overlapped with the mass of the zinc complex calculated theoretically from the elemental composition of the complex (Fig. 1). Besides the protonated molecular ion peak of the complex, the following peaks were observed at 1690, 1691, 1692, 1693, 1694, 1695, 1696, 1697 and 1698 in the high mass range representing the isotopic distribution of the metal and carbon and also different oxidation states of the zinc–ligand complexes owing to very broad isotopic distribution. Following the protonated molecular ion peak, sodium adduct peak was observed at very low intensity. Only high intense fragment peak was observed at 90 Da mass lower than the protonated molecular ion peak. This fragment ion resulted from $C_4O_2H_{10}$ elimination from the complex molecule. This fragmentation could be followed by checking the chemical structure of the zinc complex. Besides the protonated molecular ion peak and one intense fragment peak of the zinc complex, MALDI spectrum of **1** showed very clear and low fragmentation in MALDI-MS. Protonated molecular ion peak of **2** was observed at 1681 Da that was 1 Da mass higher than the protonated manganese complex calculated theoretically from the elemental composition of the complex (Fig. 2). Also the peak observed at 1682 Da has low intensity in the spectrum. All these information supported that higher oxidation states of manganese are available in the gas-phase after the laser firing under the MALDI-MS conditions. Isotopic distribution at protonated molecular ion peak region showed the isotopic pattern of the manganese addition to carbon isotopic distribution. The peak following the protonated ion peak of manganase complex represents the water adduct to the protonated complex peak. The other two higher mass peaks represented the potassium and the matrix adducts to the complex molecule. Similar MALDI-TOF results were found for cobalt porphyrazines, which confirm the proposed structure. In addition to molecular ion peaks, the peaks corresponding to the loss of $4\times H_2O$ $[M + H_2O]^+$ were easily identified.

Two principle π–π* transitions are seen for porphyrazines/phthalocyanines: a lower energy Q-band (∼550–800 nm, p–p* transition from HOMO to LUMO of the complexes) and a higher energy B-band {∼250–400 nm, deeper p–p* transition from the highest occupied MO's (a_{1u} and a_{2u}) to the LUMO (e_g)} [6]. The characteristic Q-band transition of metalloporphyrazines was observed as a single band of high intensity in the visible-region for **1**, **2** and **3** [8,13,15,18,23]. The effect of S-substitution on the periphery for all porphyrazines was a shift in these intense Q-bands to longer wavelengths when compared with those of unsubstituted and alkyl or *O*-substituted derivatives. The Q and B-bands of both the free-base and metallo compounds are greatly broadened with respect to octa-*O*-substituted porphyrazines. The broadening is attributed to n–π* transitions of the nonbonding electrons associated with the peripheral S or N atoms [11,30,35,36,37].

3.2. Spectroscopic metal ion binding titrations

It is known that macrocyclic metal complexes (MPc's) with heteroatoms fused directly to the periphery are optically sensitive to metal ions when the peripheral heteroatoms are able to interact with the metals [8–15,20–33]. Sulfur and oxygen donor atoms on the periphery of the phthalocyanines impart a preference especially for the coordination of heavy metal ions [11,15,25–31]. So, we have employed UV–vis spectroscopic titration to monitor sensing/coordinating capabilities of the MPcs for transition metal ions of Ag^{I} and Pd^{II}. Each experiment was carried out titrating THF solution of MPcs with the analyte salts of $AgNO_3$ and Na_2PdCl_4 dissolved in MeOH. Here the concentration of each MPc and the metal salt was ca 10^{-5} and 10^{-3} mol dm^{-3}, respectively.

The gradual addition (μL) of Ag^{I} to the solution of **3** at room temperature caused a color change, from blue-green to green, suggesting the complex formation of **3** with Ag^{I}. Fig. 3 shows that Ag^{I} binding to the donor atoms of **3** results in pronounced effects in the Q and B-bands, and in the n–π* transitions. This observation is in accordance with the literature [20,35,38,39]. During the titration, an intractable dark blue-black precipitate that could not be isolated formed. The addition of Ag^{I} to **3** causes a decrease in the intensity of the Q-band at 669 nm with a red shift to 675 nm. On the other hand, the B-band is accompanied by a slight blue shift (2–3 nm). These spectroscopic changes indicate the coordination of Ag^{I} by the peripheral sulfur and oxygen donor atoms of the porphyrazine. The titration measurements were also carried out for **1** and **2**, and similar changes in their spectra were obtained.

The spectroscopic changes in the titration of **3** with Pd^{II} were different when compared with that of **3** with Ag^{I}. There was a slight red shift in the Q-band at 669 nm and its intensity did not change considerably. This type of spectroscopic behavior probably results from the minor effect of Pd^{II} with respect to Ag^{I} on the aggregation–disaggregation equilibrium [39,40].

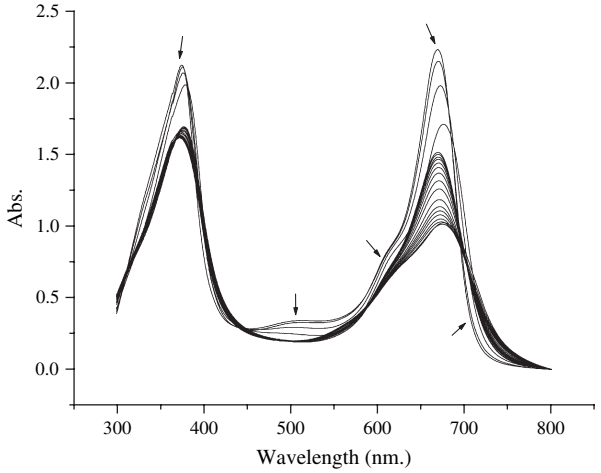

Fig. 3. UV–vis spectra during titration by Ag^{I} of **3**.

Table 1
Cyclic voltammetric parameters of complexes versus SCE

Complex	$E_{1/2}$[a] (V)	$\partial E_{p,c}/\partial \log v$ (V)	ΔE_p[b] (V)	Peak ratio[c]
H_2Pz	−0.31	0.050	0.100	0.85
	−0.62	0.050	0.105	1.10
1	−0.70	0.060	0.140	0.50
	−1.11	0.050	0.105	0.36
2	0.03	0.080	0.170	0.86
	−0.53	0.140	0.360	0.80
3	−0.10	0.050	0.105	1.10
	−0.77	0.090	0.175	0.50

[a] $E_{1/2} = (E_{p,a} + E_{p,c})/2$ for redox couple.
[b] $\Delta E_p = E_{p,a} - E_{p,c}$ at 0.100 V s^{-1} scan rate.
[c] $I_{p,a}/I_{p,c}$.

3.3. Electrochemical measurements

The electrochemical properties of the complexes were studied by cyclic voltammetry in dichloromethane, and the results are summarized in Table 1. The number of electrons transferred was determined by the CPC technique and indicated that all electron transfer processes involved one electron.

Fig. 4 shows the cyclic voltammograms of the free-base porphyrazine at different scan rates. It exhibits two ring reductions at $E_{1/2} = -0.31$ V and $E_{1/2} = -0.62$ V versus SCE. The first reduction process reveals a reversible character with a peak separation (ΔE_p) of 0.060 V at 0.010 V s^{-1} scan rate but became quasi-reversible with increasing scan rate as characterized by the variation of the cathodic peak potential with scan rate ($\Delta E_{p,c}/\Delta \log v = 0.050$ V). The second reduction process indicates very similar character with the first one as shown in Fig. 4 and in Table 1. Both ring reduction couples have simple electron transfer properties with approximately unit values of anodic to cathodic peak ratio, $I_{p,a}/I_{p,c}$.

Fig. 5 shows the cyclic voltammogram of (1.0×10^{-4} M) **1**. It displays very interesting voltammetric response. The first

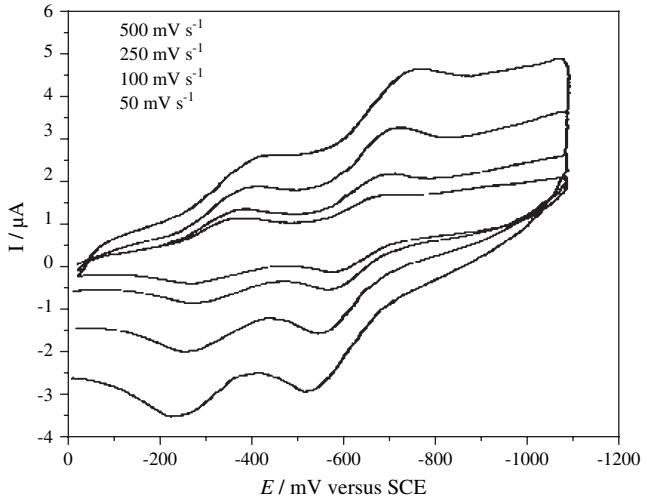

Fig. 4. Cyclic voltammograms of 2×10^{-4} M free porphyrazine at different scan rates in DMSO.

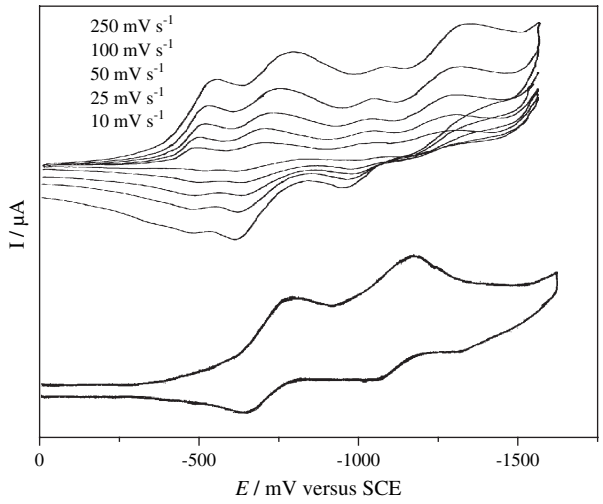

Fig. 5. Cyclic voltammograms of 10^{-4} M **1** at different scan rates in DMSO. Inset cyclic voltammogram of 5×10^{-5} M **2** at 0.100 V s^{-1} in DMSO.

reduction peak is positioned at a potential very close to the corresponding anodic wave at low scan rates. However, cathodic peak potential of the first couple shifts slightly to more negative potentials while the potential of the corresponding anodic wave does not change with scan rate. The potential difference between the first and second cathodic peaks is approximately 0.2 V although it increases slightly with scan rate. This difference is not comparable with the average separation for the first and second reduction processes of zinc–porphyrazine complexes, which is approximately 0.4 V [41]. Thus, the first two couples can be assigned to the reduction of aggregated and non-aggregated species in solution. If there is equilibrium between these species, and this equilibrium is slow relative to the electrochemical time scale, redox processes due to both species can simultaneously be observed [42,43]. Thus, the first ring reduction signal is splitted into two waves. Also, there should be aggregation–disaggregation equilibrium between the monocation species since the corresponding anodic wave for both the first and second cathodic peaks is observed during the reverse scan. This type of behavior was reported previously for an octahydroxyethyl-substituted zinc phthalocyanine complex [44]. The inset in Fig. 5 indicates the cyclic voltammogram of (5.0×10^{-5} M) **1**. As shown in this figure the splitting of reduction signals is not observed when the solution is diluted. This provides a strong evidence for aggregation–disaggregation phenomena.

The complex **2** exhibits two reductions centered at 0.03 and −0.53 V (Fig. 6). The first reduction process is expected to occur on the metal center in the first row transition metal porphyrazines because in metal "d" orbitals are usually positioned between the HOMO and LUMO of the porphyrazine ligand. This has been well established previously for tetraphenyl porphyrazines (phthalocyanines) in several papers reported by Lever et al. [6,7,30]. Thus, in the case of **2**, the first reduction is attributed to Mn(II)/Mn(I) couple while the second one is assigned to porphyrazine ring.

In the case of **1**, the first and second ring reductions were recorded at higher negative potentials than the ring reductions of the free porphyrazine. This potential difference is probably due to the variation in the effect of the interaction between the central ion and porphyrazine ring. Since ring reductions occur at more negative potentials in the case of **1**, a higher negative charge transfer should be transferred from the central ion to the ring by the replacement of two hydrogen ions with Zn(II). This negative charge transfer to the ring also occurs but more effective in the case of Mn(II) because the shift in the first ring reduction potential for **2** is higher than that for **1**. The complex **3** displays two reductions centered at −0.10 V and −0.77 V versus SCE (Fig. 7). The first reduction process which is assigned to Co(II)/Co(I) couple shows a quasi-reversible character with a peak separation of 0.105 V at 0.100 V s^{-1}. The reduction of the porphyrazine ring shows characteristics for an irreversible wave with a peak separation of 0.175 V at 0.100 V s^{-1}.

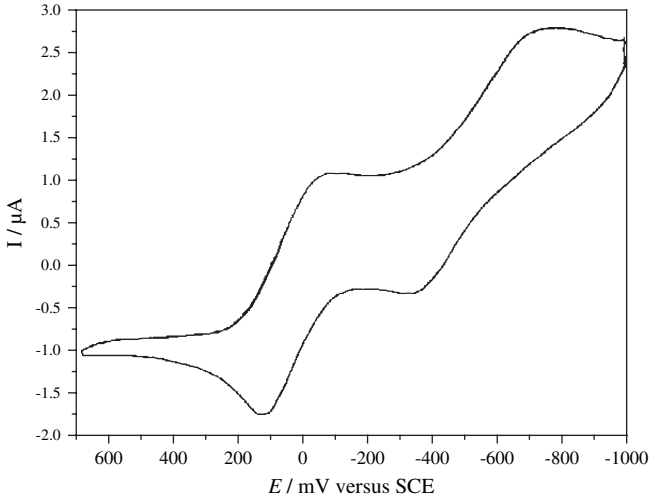

Fig. 6. Cyclic voltammogram of 2×10^{-4} M **3** at 0.100 V s^{-1} in DMSO.

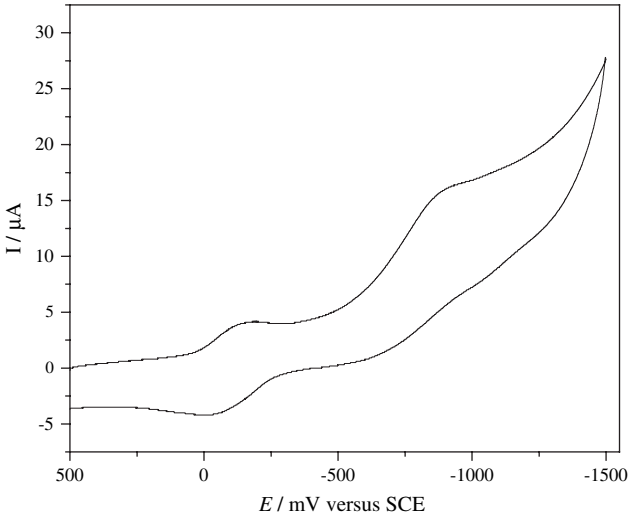

Fig. 7. Cyclic voltammogram of 2×10^{-4} M **3** at 0.100 V s^{-1} in DMSO.

Acknowledgements

We thank The Research Fund of Sakarya University (Project no: 2000-013, Project no: 2002-45), TÜBİTAK (Project no: TBAG-2241(102T167) and DPT-2004 (Project no: 2003K120970) and The Research Fund of Marmara University (Project no: SCIENCE-107/020603).

References

[1] Astruc D, editor. Electron transfer and radical processes in transition metal chemistry. New York: VCH; 1995.
[2] McKeown NB. Phthalocyanine materials. Cambridge University Press; 1998.
[3] Kahn O. Molecular magnetism. New York: VCH; 1993.
[4] Ali H, Van Lier JE. Chem Rev 1999;99:2379.
[5] Waton SP, Masschelein A, Liu S, Rebek Jr J, Lippard SJ. J Am Chem Soc 1994;116:5196.
[6] Leznoff CC, Lever ABP. In: Leznoff CC, Lever ABP, editors. Phthalocyanines: properties and applications, vols. 1–4. Weinheim: VCH; 1989–1996.
[7] Kobayashi N. In: Leznoff CC, Lever ABP, editors. Phthalocyanines properties and applications, vol. 2. New York: Wiley-VCH; 1993 [chapter 3].
[8] Kandaz M, Michel SJL, Hoffman BM. J Porphyrins Phthalocyanines 2003;7:700.
[9] Yılmaz F, Atilla D, Ahsen V. Polyhedron 2004;23(11):1931.
[10] Abdurrahmanoğlu S, Özkaya AR, Bulut M, Bekaroğlu Ö. J Chem Soc Dalton Trans 2004:4022.
[11] Kandaz M, Yılmaz I, Bekaroğlu Ö. Polyhedron 2000;19(1):115–21.
[12] Wöhrle D, Schmidt V. J Chem Soc Dalton Trans 1998:549.
[13] Baumann TF, Sibert JW, Olmstead MM, Barrett AGM, Hoffman BM. J Am Chem Soc 1994;116:2639.
[14] Donzello MP, Ou Z, Dini D, Meneghetti M, Ercolani C, Kadish KM. Inorg Chem 2004;43:8637.
[15] Ehrlich Lori A, Skrdla Peter J, Jarrel Wade K, Sibert John W, Armstrong Neal R, et al. Inorg Chem 2000;39:3963.
[16] Gross T, Chevalier F, Lindsey JS. Inorg Chem 2001;40:4762.
[17] Wöhrle D, Eskes M, Shigehara K, Yamada A. Synthesis 1993:194.
[18] Anderson ME, Barret AGM, Hoffman BM. J Inorg Biochem 2000;80:257.
[19] Fox JP, Ramdhanie, Zareba AA, Czernuszewich RS, Goldberg DP. Inorg Chem 2004;43:6600.
[20] Kandaz M, Bekaroğlu Ö. Chem Ber 1997;135:1833.
[21] Zhao M, Zhong C, Stern C, Barrett AGM, Hoffman AGM. Inorg Chem 2004;43:3377.
[22] Kobayashi N, Miwa H, Isago H, Tomura T. Inorg Chem 1999;38:479.
[23] Cook AS, Williams DBG, White AJP, Lange SJ, Stern CL, Barrett AGM, et al. Angew Chem Int Ed Engl 1997;36:760.
[24] Deng K, Ding Z, Ellis DE, Michel SJL, Hoffman BM. Inorg Chem 2001;40:1110.
[25] Michel SLJ, Barrett AGM, Hoffman BM. Inorg Chem 2003;42:814.
[26] Kandaz M, Özkaya AR, Koca A. Polyhedron 2004;29:847.
[27] Kandaz M, Özkaya AR, Koca A. Transition Met Chem 2004;29:847.
[28] Kandaz M, Özkaya AR, Cihan A. Transition Met Chem 2003;28:650.
[29] Ağırtaş MS, Sönmez M, Kandaz M, Bekaroğlu Ö. Indian J Chem Sect B 2001;40(12):1236.
[30] Kandaz M, Yaraşır MNU, Koca A, Bekaroğlu Ö. Polyhedron 2002;21:255.
[31] Hamuryudan E. Dyes Pigments 2006;68:151.
[32] Bayır ZA. Dyes Pigments 2005;65(3):235.
[33] Zhao M, Zhong C, Stern C, Barrett AGM, Hoffman AGM. Inorg Chem 2004;43:3377.
[34] Davison A, Holm RH. Inorg Synth 1967;6:8.
[35] Kandaz M, Çetin HS, Koca A, Özkaya AR. Dyes Pigments 2006; 74:298.
[36] Yilmaz I, Gürek A, Ahsen V. Polyhedron 2005;24:791.
[37] Akdemir N, Ağar E, Şaşmaz S, Gümrükçüoğlu IE, Çelebi T. Dyes Pigments 2006;69:1.
[38] Kandaz M, Bekaroğlu Ö. J Porphyrins Phthalocyanines 1999;3:339.
[39] Gürol İ, Ahsen V, Bekaroğlu Ö. J Chem Soc, Dalton Trans 1994:497.
[40] Gürek A, Bekaroğlu Ö. J Chem Soc Dalton Trans 1994:1423.
[41] Sesalan BŞ, Koca A, Gül A. Polyhedron 2003;22:3083.
[42] Bergami C, Donzello MP, Ercolani C, Monacelli F, Kadish KM, Rizzoli C. Inorg Chem 2005;44(26):9852.
[43] Piet DP, Veldhuis H, Zuilhof H, Sudholter EJR. J Porphyrins Phthalocyanines 2004;8(8):1055.
[44] Özkaya AR, Hamuryudan E, Bayir ZA, Bekaroglu Ö. J Porphyrins Phthalocyanines 2000;4(7):689.